# DECOMPOSITION OF MEASURED GROUND VIBRATIONS INTO BASIC SOIL WAVES

D. Macijauskas
*Department of Science & Technology, University of Luxembourg, Luxembourg*

S. Van Baars
*Department of Science & Technology, University of Luxembourg, Luxembourg*

**ABSTRACT:** *Man-made vibrations from different types of sources are usually measured on the surface of the ground or building. The measured signal is always the superposition of all travelling basic waves. For a homogeneous half space there are three basic waves – the Compressional (P-wave), Shear (S-wave) and Rayleigh wave (R-wave). Depending on the measuring equipment, only the accelerations or velocities in time of the superposed wave can be measured, but not the distribution of the individual basic waves.*

*Additional problems are that each of the basic waves has its own velocity, besides the body and surface waves have different attenuation laws. By using the rules of superposition of harmonic waves and also the propagation laws of the P-, S- and R-waves, it should be theoretically possible to split the measured superposed signal into the basic waves, because mathematically a system of equations can be assembled which describes the displacements at multiple measuring points in time.*

*In this paper this problem has been solved for a homogenous, elastic and isotropic soil, which is disturbed by a harmonically oscillating disc on the surface. A numerical simulation was performed using a finite element method. The displacements in time were recorded in 10 points on the surface and a system of superposed equations was assembled and solved.*

*The findings prove that each of the three basic waves has its own phase shift with the source, something which was not known before.*

## 1 INTRODUCTION

In urban areas where the infrastructure is dense and construction of new structures is near existing ones, the vibrations caused by human activities frequently occur. Generated waves in the soil may adversely affect surrounding buildings. The most known sources of the human induced vibrations are traffic (trains, buses, trucks) and civil construction activity (installation of piles, sheet piles, tunnelling, demolishing of structures, etc.). Because of environmental requirements the level of the vibrations should not exceed certain threshold values in order to protect people from discomfort, the existing structures from damage and technological processes from disturbance. This means that the level of vibration must be predicted. According to a research by Hölscher and Waarts (2003) the reliability of prediction methods is disappointingly low, so it is evident that the soil models for vibrations should be improved first in order to get more accurate predictions.

According to theory, the vibrations in a homogeneous half space are complex superposed waves, made up of body and surface waves, which are the following three basic waves – the Compressional (P-wave), Shear (S-wave) and Rayleigh wave (R-wave). These three basic

waves have different attenuation, different propagation laws (wave speed) and different damping laws. The attenuation and propagation laws have been solved already, but the damping laws are still subject of study.

Bolton & Wilson (1990) concluded from cyclic tests on sand that the stress-strain behaviour of the soil is hysteretic and its corresponding damping parameters are strain dependent, though they are independent of the frequency up to 100 Hz. Van Baars (2011) noticed that man-made vibrations result in shear deformations with an amplitude no greater than $\hat{\gamma} = 0.01$. Van Baars used results from other researchers (Okur & Ansal, 2007, for instance) to demonstrate that fortunately the damping ratio is nearly constant up to this magnitude. Hysteretic damping is in fact a damping resulting from frictional shear deformation. Isotropic compression causes probably little or no damping.

In P -waves there is a deformation due to mostly isotropic compression but also some shear deformation, in S-waves there is only pure shear deformation and in R-waves there is a combination of mostly shear deformation but also deformation due to isotropic compression. Therefore the energy in the basic waves will not only attenuate differently and propagate differently, but also damp differently.

So, in order to have a better insight into the propagation of vibrations in a soil medium, the measured signal has to be decomposed into the basic waves and analysed separately. A main problem in the field is that, not independent waves are measured, but only superposed velocities or accelerations. So in order to study the measurements, a way to decompose the superposed waves into basic waves, should be found first.

## 2 DECOMPOSITION OF WAVES

In this paper this problem has been solved for a homogenous, elastic and isotropic soil, which is disturbed by a harmonically oscillating disc on the surface, see Figure 1.

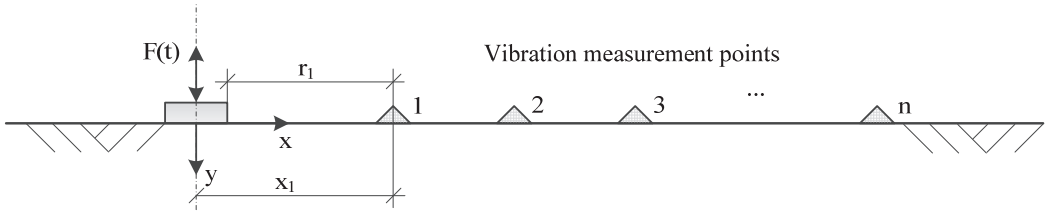


Fig. 1. Sketch of an oscillating plate and measurement points

The displacement of each point on the soil surface in direction *i* can be described as a superposition of the displacements of the three basic waves in that point:

$$u_i(r,t) = u_{p,i}(r,t) + u_{s,i}(r,t) + u_{r,i}(r,t) \tag{1}$$

where $u_{p,i}$, $u_{s,i}$, $u_{r,i}$, are the displacements of the P-, S- and R-wave respectively.

By taking into account the propagation laws of the general waves, Equation (1) can be rewritten for any measurement point as follows:

$$\begin{aligned} u_x(r,t) &= \hat{u}_{p,x}\sin\left(\omega t - k_p r - \Delta\phi_p\right) + \hat{u}_{s,x}\sin\left(\omega t - k_s r - \Delta\phi_s\right) - \hat{u}_{r,x}\cos\left(\omega t - k_r r - \Delta\phi_r\right) \\ u_y(r,t) &= \hat{u}_{p,y}\sin\left(\omega t - k_p r - \Delta\phi_p\right) + \hat{u}_{s,y}\sin\left(\omega t - k_s r - \Delta\phi_s\right) + \hat{u}_{r,y}\sin\left(\omega t - k_r r - \Delta\phi_r\right) \end{aligned} \tag{2}$$

where $\hat{u}_{j,i}$ is the amplitude of the $j$ wave in the $i$ direction, $\omega$ is the angular frequency of the harmonic wave, $k_j$ is the $j$ wave's number, $\Delta\phi_j$ is the phase shift of a the $j$ wave.

In order to relate the measured vibrations of the different points with different distances, the attenuation laws of the basic waves will be used. The amplitudes of the body waves (P- and S-waves) attenuate proportional to $x^{-1}$ and the surface wave (R-wave) attenuates proportional to $x^{-1/2}$, where $x$ is the distance from the axis of symmetry, which is the middle of the disc (Fig. 1). For relatively small discs follows $x = r$. Now vibrations in any measurement point $i = 1...n$ can be expressed as functions of amplitudes in any other point, for example the 1st point:

$$\begin{aligned} u_{x,i}(r,t) &= \hat{u}_{p,x,1}\sin\left(\omega t - k_p r_i - \Delta\phi_p\right)\frac{x_1}{x_i} + \hat{u}_{s,x,1}\sin\left(\omega t - k_s r_i - \Delta\phi_s\right)\frac{x_1}{x_i} \\ &\quad -\hat{u}_{r,x,1}\cos\left(\omega t - k_r r_i - \Delta\phi_r\right)\sqrt{\frac{x_1}{x_i}} \\ u_{y,i}(r,t) &= \hat{u}_{p,y,1}\sin\left(\omega t - k_p r_i - \Delta\phi_p\right)\frac{x_1}{x_i} + \hat{u}_{s,y,1}\sin\left(\omega t - k_s r_i - \Delta\phi_s\right)\frac{x_1}{x_i} \\ &\quad +\hat{u}_{r,y,1}\sin\left(\omega t - k_r r_i - \Delta\phi_r\right)\sqrt{\frac{x_1}{x_i}} \end{aligned} \tag{3}$$

The back-calculated superposed signal can be used as a check, as well as the theoretical ratio of the R-wave's amplitudes on the surface $\hat{u}_{r,x,i} / \hat{u}_{r,y,i}$ .

## 3 NUMERICAL SIMULATION

In order to check this technique, a 2-dimensional, axial symmetrical numerical simulation was performed with the Finite Element Method software Plaxis. The advantage of a numerical simulation is that the material damping can be put to zero. The general force-displacement matrix in Plaxis is based on the following equation:

$$[M]\{\ddot{u}\} + [C]\{\dot{u}\} + [K]\{u\} = \{F\} \tag{4}$$

where $[M]$ is the mass matrix, $\{u\}$ is the displacement vector, $[C]$ is the damping matrix, $[K]$ is the stiffness matrix and $\{F\}$ is the load vector. First and second derivatives of displacement vector are velocity and acceleration vectors respectively.

The damping matrix $[C]$ represents the material damping. In Plaxis 2D, Rayleigh damping is used, where $[C]$ is a function of the mass and stiffness matrices, according:

$$[C] = \alpha[M] + \beta[K] \tag{5}$$

where $\alpha$ and $\beta$ are coefficients, which are kept zero in this simulation, to avoid any type of material damping.

The used geometry and mesh of the model can be found in Figure 2. The model is 50 m in length and width. The 10 measurement points for displacement recording were placed from 15 m to 24 m, at 1 m distance from each other. The soil is modelled with 15-node elements having a Young's modulus $E$ = 51.02 MPa and a Poisson's ratio $\nu$ = 0.25. The oscillating

disc has a radius of 0.2 m, which is modelled with a plate element with stiffness $EI = 24$ MNm$^2$/m. First the disc is loaded with a static load of 20 kPa and later a harmonic load of ±10 kPa at 10 Hz is introduced.

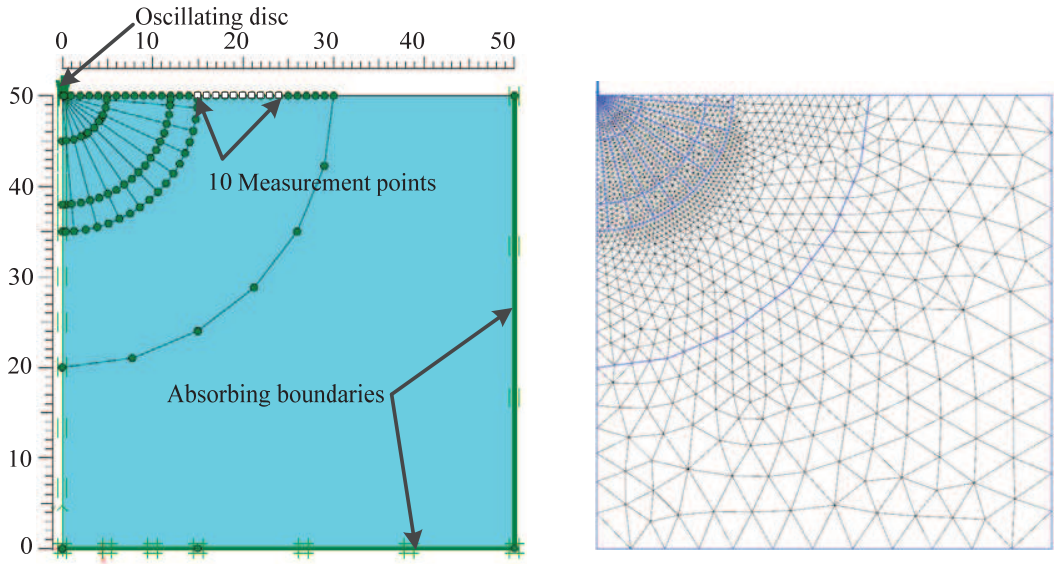


Fig. 2. Geometry and mesh of the FEM model

## 4 RESULTS

The displacements were first used after about 3 cycles, so that the starting up effect of the harmonic load has vanished. The time window for the measurement was also selected such that are no reflections yet from the absorbing boundaries, since they do not absorb perfectly.

### *4.1 First attempt*

The idea of the first attempt was to use only the displacements which were measured at a selected time when the displacement reached a peak. It was assumed that the three basic waves were in phase with the original/superposed wave, similar as in the analytical solution of Miller and Pursey (1955).

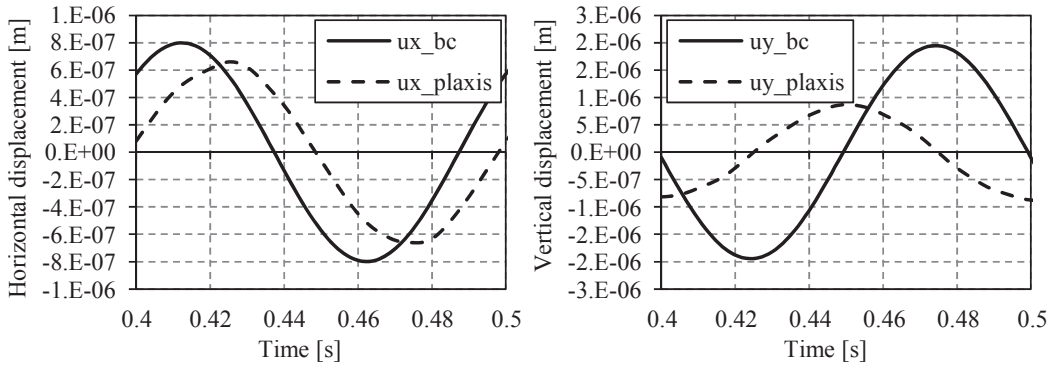


Fig. 3. First attempt: back-calculated results vs. Plaxis

The correlation factors are very low. The factor of the vertical component even becomes negative, which means there is no good solution. Also the ratio of the R-wave's amplitudes $\hat{u}_{r,x,i} / \hat{u}_{r,y,i}$ = 3.73 which is much greater than the theoretical $\hat{u}_{r,x,i} / \hat{u}_{r,y,i}$ = 0.682.

Only for the selected time (the peak of the dashed line) the solution almost fitted, but clearly not for the rest of the wave.

### *4.2 Attempt with phase shifts*

A new attempt was done, but this time with allowing the basic waves to have different phases as the original/superposed wave. This leads to nine unknowns (six amplitudes and three phase shifts). Since the phases of the basic waves are now unknowns, the system of equations is not linear anymore, so the solution had to be found by using the least square method in an iterative way. In this attempt not only the peak values of the time-displacement graph, but all values of one cycle were used. One cycle $T$ = 0.1 s. The calculations were performed with time steps of $\Delta t$ = 0.001 s, which gives 100 time steps or points in a time-displacement graph. Since there are 10 measurement points with each 2 equations (horizontal and vertical); there is a system of 2000 equations. The horizontal and vertical displacements of the basic waves were solved and are shown in Figure 4.

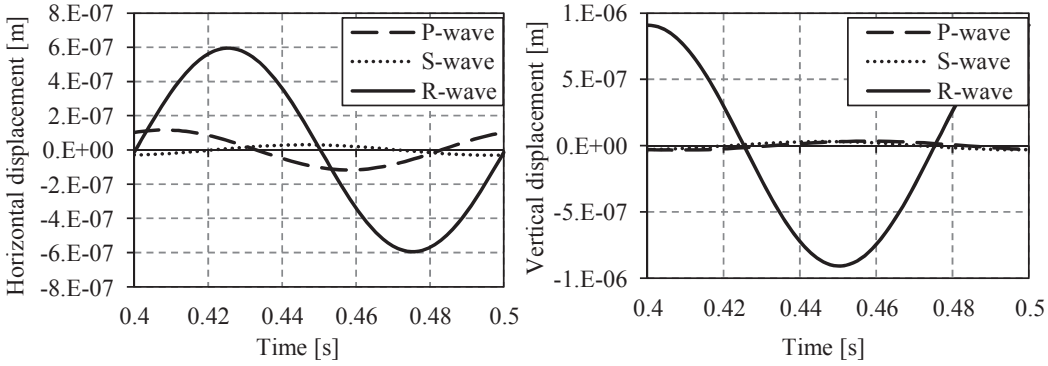


Fig. 4. Phase shifts: horizontal and vertical displacements of the basic waves

This time a perfect fit of the wave displacements was found for the back calculated wave with the recorded wave of Plaxis. The correlation factor $R^2$ is equal to 0.9986 for the combined displacements.

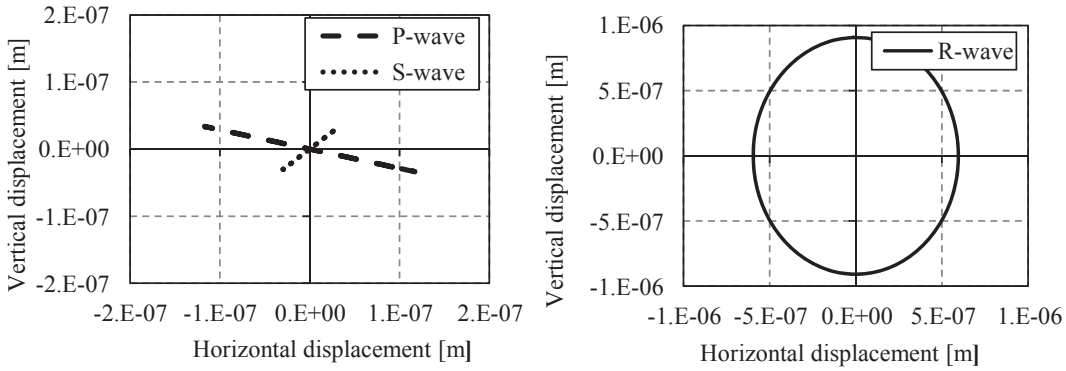


Fig. 5. Phase shifts: displacements on the surface of one cycle of the three basic waves

Figure 5 shows the displacements on the surface of one cycle of the three basic waves in point 1. Interesting is to note that both the P-wave and the S-wave do not act completely flat (horizontal for the P-wave and vertical for the S-wave). Also interesting is the ratio of the R-wave's amplitudes is found to be $\hat{u}_{r,x,i} / \hat{u}_{r,y,i} = 0.655$, which is in a quite good agreement with the theoretical $\hat{u}_{r,x,i} / \hat{u}_{r,y,i} = 0.682$.

### *4.3 Attempt with flat waves*

The same attempt was done, but this time with the assumption that the body waves are flat, so the horizontal amplitude of the S-wave and the vertical amplitude of the P-wave are zero. Also the ratio of the theoretical R-wave's amplitudes was used, so $\hat{u}_{r,x,i} / \hat{u}_{r,y,i} = 0.682$. This reduces the amount of unknowns back to six (three amplitudes + three phase shifts).

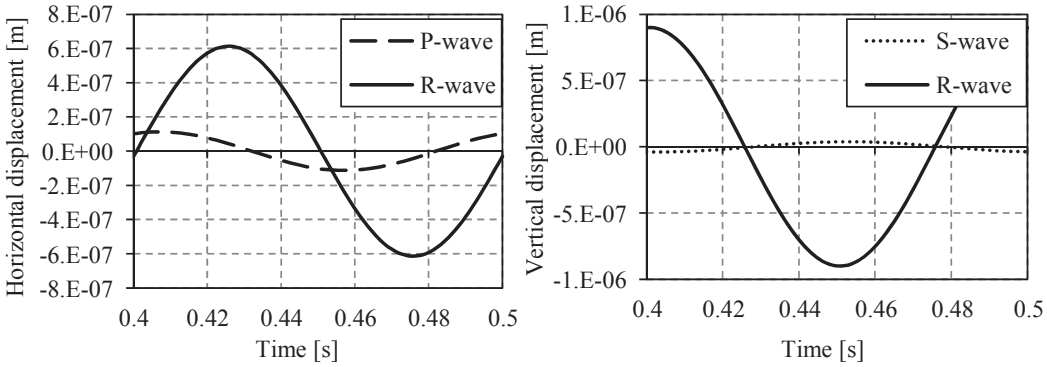


Fig. 6. Flat waves: horizontal and vertical displacements of the basic waves

Figure 6 shows the displacements on the surface of one cycle of the three basic waves in point 1.

Table 1. Effect of the reduction of unknowns

| Wave | Direction | Unknown | 9 unknowns | 6 unknowns | Units |
|---|---|---|---|---|---|
| P | h | $A_{px}$ | 0.117 | 0.113 | $[m \cdot 10^{-6}]$ |
| S | v | $A_{sy}$ | 0.031 | 0.039 | $[m \cdot 10^{-6}]$ |
| R | h | $A_{rx}$ | 0.595 | 0.614 | $[m \cdot 10^{-6}]$ |
| P | v | $A_{py}$ | -0.034 | - | $[m \cdot 10^{-6}]$ |
| S | h | $A_{sx}$ | 0.030 | - | $[m \cdot 10^{-6}]$ |
| R | v | $A_{ry}$ | 0.908 | from ratio | $[m \cdot 10^{-6}]$ |
| P | - | $\Delta\varphi_p$ | -8.7 | -12.1 | [deg] |
| S | - | $\Delta\varphi_s$ | -96.1 | -71.1 | [deg] |
| R | - | $\Delta\varphi_r$ | 51.9 | 53.5 | [deg] |
| Ratio of the R-wave amplitudes | | | | | |
| | | $A_{rx} / A_{ry}$ | 0.655 | 0.682 | [ - ] |
| | | mean($R^2$) | 0.9986 | 0.9982 | |

Forcing the body waves to be flat and the ratio of R-wave's amplitudes to be as the theoretical one, did not change the correlation factor very much. The combined mean

correlation factor for the horizontal and vertical displacements is still very high $R^2 = 0.9982$. The amplitudes and phase shifts are shown in Table 1. For most of them the difference is rather small, except for the S-wave's phase shift, which was found to have a difference of 25°.

The basic waves are shown in Figure 7 for one cycle when the soil body oscillates harmonically. As can be seen, the P- and S-waves are prior to the disc loading, but the R-wave is delayed. The values of the phase shifts shown in Figure 7 are the ones of Table 1.

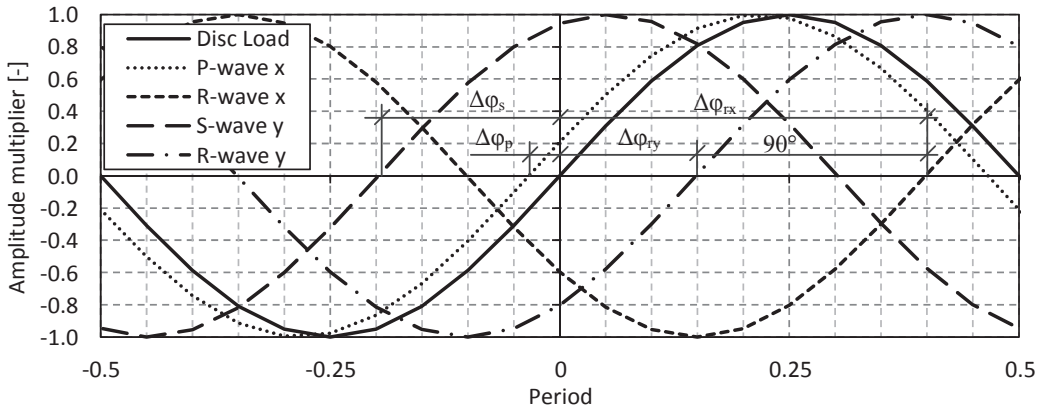


Fig. 7. Phase shifts of the basic waves

## 5 ENERGY BALANCE

Since the wave is now decomposed, the energy balance can be checked. Since there is no material damping, the emitted energy from the oscillating disc on the surface and the energy carried by the basic waves should be in balance (principle of energy conservation).

### *5.1 Total Energy*

First of all the energy emitted from the source was calculated. For displacement recordings one point on the disc was selected. One point is sufficient, because the disc is stiff enough, so its own deformations are negligible.

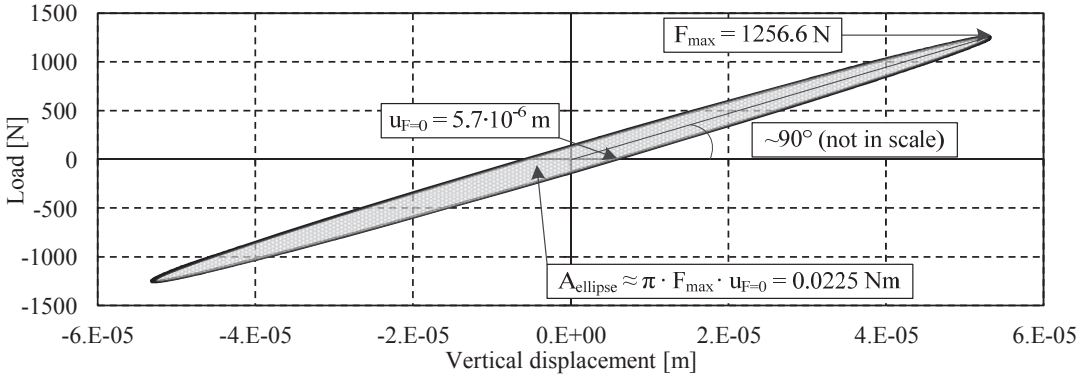


Fig. 8. Total emitted energy per cycle

The emitted energy per cycle from the oscillating disc was calculated from the load-displacement ellipse, which represents the work per cycle (Fig. 8). The total emitted energy was found to be 0.0225 Nm per cycle.

*5.2 Energy in the basic waves*

The energy in the R-wave was calculated by using the analytical solution of the R-wave's amplitudes in depth. These functions can be found in books of soil dynamics, like Kramer (1996), for instance. In order to estimate the total energy in the R-wave per cycle $E_{tot,r}$, the functions of the squared amplitudes (energy is proportional to the squared of the amplitudes) are integrated over depth for one wave length:

$$E_{tot,r} = \frac{1}{2}\rho\omega^2(2\pi r\lambda_r)\int_{y=0}^{y=\infty}(\hat{u}_x^2 + \hat{u}_y^2)dy \tag{6}$$

where $\rho$ is the density of the medium, $\omega$ is the angular frequency of the harmonic wave, $\hat{u}_x$, $\hat{u}_y$ are the amplitudes of the R-wave in x and y direction respectively, $r$ is the radius, $\lambda_r$ is the length of the R-wave.

Unfortunately the analytical amplitude functions of the P- and S-waves, used by Miller and Pursey (1955), exist only for a very large radius, where the amplitudes are equal to zero on the surface. This is clearly not the case here. Therefore first the amplitude functions of the P- and S-waves have to be constructed.

Therefore the displacements were recorded in 19 additional points, placed in the soil volume (see Fig. 9 on the left). By using the amplitudes of the R-wave at the surface and the theoretical amplitude functions in depth, the displacements of the R-wave were calculated for the same 19 points. These displacements in time of the R-wave were subtracted from the recorded total displacements. The residual displacements in x and y directions were projected onto the x' and y' axis (see Fig. 9 on the right), which are the directions of the motion of an individual particle of the P- and S-waves, respectively. In this way, for the P- and S-waves, the amplitudes of the displacements in x' and y' axes were calculated.

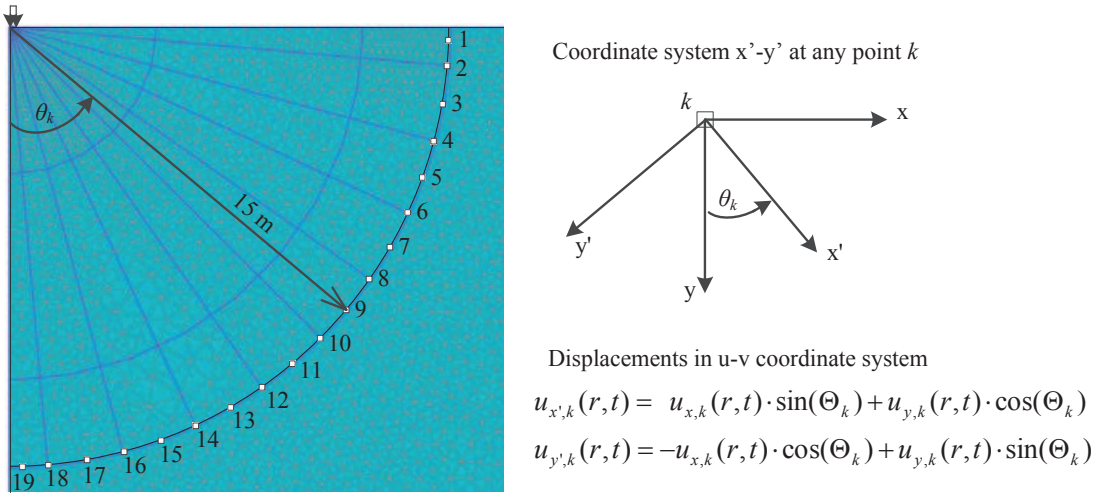


Fig. 9. Additional points for the amplitudes of S- and P-waves

The total energy in the P- (or S-wave) per cycle $E_{tot,p(s)}$ can be calculated by integrating the squared functions of the amplitudes (energy is proportional to the squared of the amplitudes) over a surface of a half ball for one wave length:

$$E_{tot,p(s)} = \frac{1}{2}\rho\omega^2\left(2\pi r\lambda_{p(s)}\right)\int_{\Theta=0}^{\Theta=\pi/2}\left(\hat{u}^2_{p(s)}\cdot\sin\Theta\cdot r\right)d\Theta \tag{7}$$

where $\lambda_{p(s)}$ is the P- (or S-wave's) wave length, $\hat{u}_{p(s)}$ is the amplitude of the P- (or S-wave), $\Theta$ is the polar angle.

The total amount of energy carried by the basic waves was summed and found to be 0.0224 Nm per cycle, which is almost the same as the total emitted energy of 0.0225 Nm per cycle.

### *5.3 Distribution of Energy in Waves*

Also the distribution of the total energy in the basic waves was checked. This problem was solved analytically by Miller and Pursey (1955), for a soil with Poisson's ratio $\nu$ = 0.25, but this has never been checked numerically. The percentages of the total energy distribution in the basic waves can be found in Table 2.

Table 2. Distribution of the total energy in the basic waves

| Solution | P-wave [%] | S-wave [%] | R-wave [%] |
|---|---|---|---|
| Analytical | 6.9 | 25.8 | 67.4 |
| FEM | 10.8 | 28.5 | 60.7 |

As can be seen from this table, the distribution of the energy based on the analytical solution of Miller and Pursey fits reasonably well to the numerical solution, despite the fact that Miller and Pursey were not aware of the phase shifts of the basic waves. The small differences could be explained by different initial conditions between the solutions. First, in the analytical solution no phase shifts were considered. Second, a very small and flexible disc with infinite small radius was used, while in the numerical simulation a rigid disc was used. Third, numerical methods always have residual errors.

## 6 CONCLUSIONS

The example in this article discusses a harmonically oscillating disc on a homogeneous half space. The recorded superposed soil wave can be decomposed into its basic waves when multiple geophones are used. From the recorded data a system of non-linear equations can be assembled with six unknown parameters (three amplitudes and three phase shifts). These six parameters can be solved by using an iterative way of the least square method. This leads to a decomposition into the three basic waves, with each its own amplitude and phase shift. The superposition of only these basic waves describes very accurately the recorded superposed soil wave, proofing the existence of only three basic waves. The findings proof also that all three basic waves have phase shifts and these phase shifts are all different from each other. Both facts were not known before. Although it is important to notice the existing of the individual phase shifts, it is still not clear what causes them.

An energy balance showed that the amount of emitted energy by the load on the disc is the same as of the sum of energies of the basic waves. This is another type of evidence that only

three basic waves exist. The distribution of the energy over the three basic waves based on the analytical solution of Miller and Pursey (1955) fits reasonably well to the numerical solution shown in this article, despite the fact that Miller and Pursey were not aware of the phase shifts of the basic waves. The major part of the energy (more than 60 %) from a vertically oscillating disc on the surface goes into the R-wave.

## REFERENCES


**Journal**

Okur, D.V. & Ansal A. (2007), "Stiffness degradation of natural fine grained soils during cyclic loading", Soil Dynamics and Earthquake Engineering, Vol. 27(9), 843-854.

**Book**

Kramer, S.L. (1996), Geotechnical Earthquake Engineering. Prentice Hall, New Jersey.

**Proceedings**

Bolton M.D. & Wilson J.M.R. (1990), "Soil stiffness and damping", Proceedings of The International Conference on Structural Dynamics, Eurodyn '90, University of Bochum, 1, 209-216,

Miller, G.F. & Pursey, H. (1955), "On the Partition of Energy between Elastic Waves in a Semi-Infinite Solid", Proceedings of the Royal Society of London. Series A, Mathematical and Physical Sciences, Vol. 233(1192), 55-69.

Van Baars, S. (2011), "Modelling of frictional soil damping in finite element analysis", Proceedings of The Second International Symposium on Computational Geomechanics, Croatia, ISBN 978-960-98750-1-1, April 2011.

**Other**

Hölscher, P. & Waarts, P. H. (2003), "Reliability of vibration prediction and reducing measures", Final Report. Delft Cluster, Delft.